Phase Behavior of Cured and Uncured Propoxylated Glyceroltriacrylate/ 8CB Mixtures

Ulrich Maschke,*,† Farida Benmouna,‡,§ Frédérick Roussel,|| Abdelylah Daoudi,|| Frédéric Gyselinck,† Jean-Marc Buisine,|| Xavier Coqueret,† and Mustapha Benmouna‡,§

Laboratoire de Chimie Macromoléculaire−CNRS (UPRESA 8009), Bâtiment C6, Université des Sciences et Technologies de Lille, F-59655 Villeneuve d'Ascq, France; Max-Planck-Institut für Polymerforschung, Postfach 3148, D-55021 Mainz, Germany; and Laboratoire de Thermophysique de la Matière Condensée−CNRS (Equipe de l'UPRESA 8024), Université du Littoral, MREID, F-59140 Dunkerque, France

Received August 16, 1999; Revised Manuscript Received October 25, 1999

ABSTRACT: Uncured and cured propoxylated glyceroltriacrylate (GPTA)/4-cyano-4′-*n*-octyl-biphenyl (8CB) mixtures were prepared. The cured samples have been obtained by polymerization/cross-linking reactions using electron-beam irradiation. All cured samples with different compositions were exposed to the electron beam under similar conditions keeping the same dose and dose rate. The phase behavior of cured and the corresponding uncured GPTA/8CB mixtures was established by combining polarized optical microscopy and differential scanning calorimetry. The coexistence curve describing transitions from ordered to isotropic phase is analyzed using a theoretical framework in which the smectic-A and nematic order is described by a generalization of the Maier−Saupe theory developed by McMillan.

Introduction

Mixtures of polymers and liquid crystals (LCs) are interesting not only from the fundamental point of view but also from the numerous applications.[1−4] A particular class of these systems are commonly referred to as PDLCs (polymer dispersed liquid crystals).[3−7] In general, PDLC systems are thin films that consist of micrometer-sized droplets of ordered LC molecules in a solid polymer matrix. One of the main applications of these films is related to their particular electrooptical properties. Indeed, they can be electrically switched from an opaque off-state to a transparent on-state. The thermodynamic properties of these systems determine to a large extent the degree of opacity in the off-state and transparency in the on-state, which makes knowledge of these properties crucial.

Until recently, equilibrium phase behavior has been investigated mainly in the case of PDLC systems made of linear polymers and low-molecular-weight LC (LMWLC). Nwabunma and Kyu reported the phase diagram of NOA65/LC in the uncured[8] and in the UV-cured[9] state. The latter system has been prepared by a polymerization induced phase separation (PIPS) process induced by UV light, starting from the commercial reactive mixture NOA65 and leading to a cross-linked network. The nematic LC mixed with this polymer was K21, which has a nematic−isotropic transition temperature $T_{NI} = 42.8$ °C.

In the present paper, the equilibrium phase diagram of mixtures of propoxylated glyceroltriacrylate (GPTA) and 4-cyano-4′-*n*-octyl-biphenyl (8CB) has been explored by polarized optical microscopy (POM) and differential scanning calorimetry (DSC). The phase diagram in the cured state has also been established. In this case, the polymer matrix is prepared by a PIPS process using electron-beam (EB) radiation. This technique was already confirmed as a powerful method to obtain well-defined PDLC films.[5,7] Compared with the PIPS process by UV light, EB curing of acrylate materials has the unique advantage of not requiring the presence of a photoinitiator, which may be detrimental to PDLC film performance and long-term aging.

The LMWLC used in this study is 8CB, which is a pure LC characterized by widely different transition temperatures from smectic-A to nematic and nematic to isotropic states. Investigation of the phase behavior of this system is favorable because it is made of only two molecular species, thus avoiding the complexities inherent in multicomponent systems. This is particularly useful for a better characterization of the effects of cross-links on the phase behavior of polymer and LC systems.

This is the first time that a phase diagram of cross-linked polymer prepared by EB radiation and smectic-A LMWLC is reported. The experimental data are analyzed using a theoretical framework describing mixtures of cross-linked polymers and LMWLC in the isotropic state and in the smectic-A order. The phase behavior in the isotropic state of such systems is a well-documented problem in the literature. Here, we use a model for the elastic free energy of the network based on the Flory−Rehner theory of elasticity.[10−16] The rubber elasticity parameters and the Flory−Huggins interaction parameters are allowed to be function of the polymer volume fraction in order to obtain a good agreement with the experimental data. To describe the smectic-A order, the extension of the Maier−Saupe theory of nematic order due to McMillan is employed.[17−19] A theoretical framework combining the Flory−Rehner theory of elasticity described earlier and the Maier−Saupe−McMillan theory of nematic and smectic-A

* To whom correspondence should be addressed. E-mail: maschke@univ-lille1.fr.
† Université des Sciences et Technologies de Lille.
‡ Max-Planck-Institut für Polymerforschung.
§ Permanent address: Institute of Physics and Chemistry, University Aboubakr Belkaïd of Tlemcen, Algeria.
|| Université du Littoral.

10.1021/ma991389h CCC: $18.00
Published on Web 11/25/1999

orders has already been applied to various mixtures involving cross-linked polymers and LMWLC.[20−22] It was shown that several parameters influence the phase properties of these mixtures, and the analysis is somewhat more complicated than in the case of linear polymer systems. Those theoretical studies provide useful guides for the choice of parameters to fit the experimental data of real systems.

Experimental Section

a. Materials. Propoxylated glyceroltriacrylate (GPTA) as monomer was donated from Cray Valley (France) and used without purification. The LC is 4-cyano-4′-*n*-octyl-biphenyl or 8CB showing a smectic-A order. It was purchased from Frinton Laboratories (New Jersey) and presents in the pure state characteristic transition temperatures that were provided by the manufacturer as follows: $T_{KS} = 21.5$ °C, $T_{SN} = 33.5$ °C, and $T_{NI} = 40.5$ °C.

b. Sample Preparation. Mixtures of $(100 - x)$ weight percent (wt %) of the monomer ($x = 10, 20, ..., 90$) and x wt % of 8CB were stirred mechanically at room temperature for several hours. Two series of samples have been prepared, the first consisting of the reactive initial mixtures and the second including the same compositions but in the cured state:

Reactive Mixtures. A small amount of the initial reactive mixture was sandwiched between two glass slides. The same procedure was repeated to have two or more samples at the same composition prepared independently to check for reproducibility of the results.

For the DSC measurements, the samples were prepared by introducing approximately 3 mg of the initial mixture into aluminum DSC pans.

Cured Samples. In the case of microscopy observations, the thickness and the uniform application of the reactive initial mixtures on glass slides was controlled by using a wire-wound rod as a bar coater of 10 μm (Braive, Belgium). For each composition, several samples have been prepared and exposed to the electron-beam radiation to cure the polymerizable mixture.

Samples used for DSC measurements could be realized by uniform application of the reactive mixtures on aluminum sheets as supports, using a bar coater of 75 μm.

c. Electron-Beam Curing. The electron-beam cure technique was employed in order to prepare the PDLC samples by a PIPS process. The generator used in our experiments was an Electrocurtain model CB 150 (Energy Sciences Inc.) with an operating high voltage of 175 kV.

The sample placed in a nitrogen atmosphere is submitted to the accelerated electron curtain. The conveyor entrance was equipped with a reverse nitrogen stream to avoid changes of the inertization conditions.

The glass slides prepared as mentioned above were placed in a sample tray. This tray was passed under the electron curtain on a conveyor belt. The amount of energy required to cure products is called the dose. In our experiments, the dose applied was 104 kGy. This was achieved by using a beam current of 7 mA and a conveyor speed of 0.19 m/s. These values have not been changed during our experiments in order to apply each time the same curing conditions. No temperature control during the irradiation process has been performed. Because our sample thickness did not exceed 75 μm, the dose was essentially delivered in an uniform way.

d. DSC Measurements. DSC measurements were performed on an apparatus of the type SEIKO DSC 220C equipped with a liquid nitrogen system and allowing for cooling and heating ramps. The apparatus cell was purged with nitrogen at a rate of 50 mL/min. The same heating−cooling ramps were used for the microscopy measurements in the temperature range −100 to +100 °C. Data were recorded systematically on the second heating ramp.

e. POM Measurements. The polarized optical microscope (POM) used in this study is of type Leica DMRXP, equipped with a heating−cooling stage Linkam THMSE 600. Samples were heated at the rate 2 °C/min from room temperature to 15 °C above the transition temperature leading to the isotropic phase. Then, samples were left approximately 5 min in the isotropic state. Afterwards, the samples corresponding to 50 wt % 8CB or higher were cooled to room temperature at a rate of −2 °C/min. For the other samples with low concentration in LC, cooling was performed to $T = -10$ °C to allow for phase separation and formation of ordered regions if a LC phase does exist. This procedure is followed after 5 min by a heating ramp at a rate of 2 °C/min. Transition temperatures were recorded during the heating ramp.

Theoretical Background

A theory of the phase behavior of smectic-A LC and linear polymers has been described by Kyu et al.[23−26] by combining the Flory−Huggins and the Maier−Saupe−McMillan theories. Extension of this theory to systems involving cross-linked polymers has revealed interesting differences due to the elastic forces introduced by the cross-links, which resists the swelling of the polymer.[21]

The free energy density of the mixture can be written as a sum of two contributions

$$f = f^{(i)} + f^{(s)} \tag{1}$$

where the superscripts i and s refer to isotropic and smectic-A, respectively. Within the Flory−Rehner theory of rubber elasticity,[10,11] the isotropic free energy of the system is

$$\frac{f^{(i)}}{k_B T} = \frac{3\varphi_r^{2/3}\alpha}{2N_c}[\varphi_2^{1/3} - \varphi_2] + \frac{\beta\varphi_2}{N_c}\ln\varphi_2 + \frac{\varphi_1 \ln \varphi_1}{N_1} + \chi\varphi_1\varphi_2 \tag{2}$$

where k_B is the Boltzman constant, T is the absolute temperature, φ_r is the reference state polymer volume fraction, N_c is the number of repeat units between consecutive cross-links, and α and β are the model-dependent rubber elasticity parameters. φ_1 and φ_2 are the volume fractions of LMWLC and polymer, respectively. Assuming incompressibility and equality of molar volumes of species 1 and 2, one has $\varphi_1 = 1 - \varphi_2$. The LMWLC is supposed to have a single repeat unit which means that $N_1 = 1$.

The isotropic free energy is the main source of difference between the thermodynamic properties of mixtures with either linear or cross-linked polymers. The presence of cross-links introduces remarkable differences between the phase behavior of uncured and cured samples. The free energy arising from the nematic and the smectic-A orders is the same for uncured and cured systems.

Within the Maier−Saupe−McMillan[17−19] theory, one writes

$$\frac{f^{(s)}}{k_B T} = \frac{\varphi_1}{N_1}\left[-\ln Z + \frac{1}{2}\nu\varphi_1(S^2 + \zeta\sigma^2)\right] \tag{3}$$

where Z represents the partition function

$$Z = \int\int d\mu\, dz \exp\left[\frac{m_n}{2}(3\mu^2 - 1)\right] \times \exp\left[\frac{m_s}{2}(3\mu^2 - 1)\cos 2\pi\frac{z}{d}\right] \tag{4}$$

The integration over μ is performed in the range [0,1],

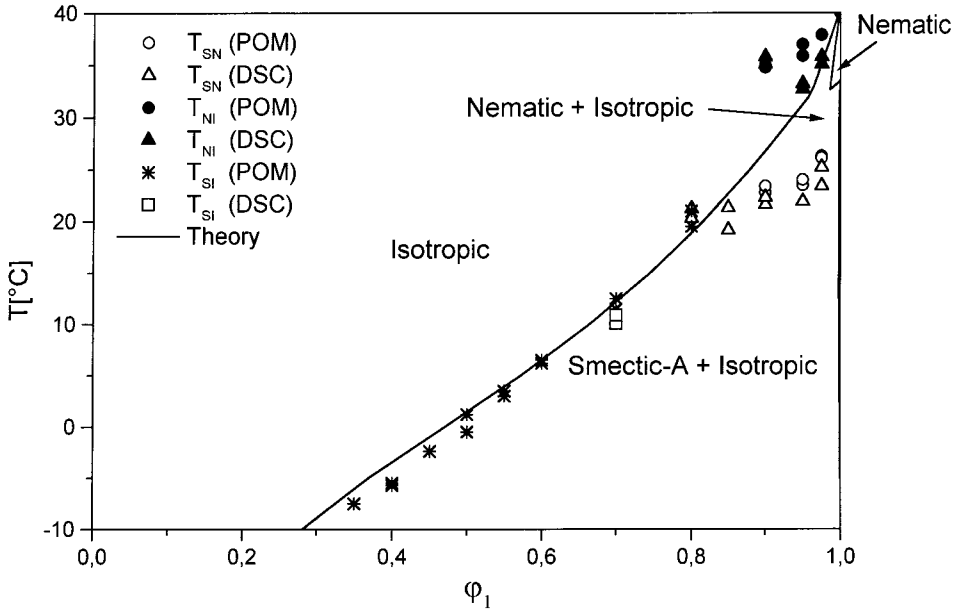

Figure 1. Equilibrium phase diagram of uncured GPTA/8CB samples. The symbols represent experimental data obtained by POM and DSC as indicated on the diagram. The solid line is the theoretical coexistence curve obtained using the following parameters: $N_1 = 1$, $N_2 = 2$, $\chi = -6.075 + 1861/T$, $T_{SN} = 33.5$ °C, $T_{NI} = 40.5$ °C, and $\zeta = 0.9375$.

whereas the integration over z should be made in the range $[0,d]$ and normalized with respect to d, the interlayer spacing along the z-axis in the smectic-A ordering. S is the nematic order parameter

$$S = \frac{1}{2}\langle 3\cos^2\theta - 1\rangle \tag{5}$$

and σ is the smectic-A order parameter along the z-direction

$$\sigma = \frac{1}{2}\left\langle \cos\frac{2\pi z}{d}(3\cos^2\theta - 1)\right\rangle \tag{6}$$

The symbol $\langle ... \rangle$ represents the average with respect to the equilibrium distribution function. $\nu = 4.54(T_{NI}/T)$ is the Maier−Saupe quadrupole interaction parameter for nematic ordering. According to the McMillan theory, ζ depends on the transition temperatures T_{SN} and T_{NI} of the LC. For 8CB, ζ is found to be 0.9375. The interaction strengths relative to the nematic and the smectic-A orders m_n and m_s are mean field parameters obtained from minimization of the free energy with respect to S and σ

$$m_n = \nu S\varphi_1 \quad \text{and} \quad m_s = \zeta\nu\sigma\varphi_1 \tag{7}$$

Results and Discussion

Uncured Samples. The equilibrium phase diagram of the uncured GPTA/8CB mixtures is shown in Figure 1. The symbols are data obtained by optical microscopy and DSC. This diagram shows three regions. A wide region exists exhibiting a single isotropic phase. This region covers a large domain on the temperature−composition diagram expressing the high degree of miscibility of the two low-molecular-weight species. There is a biphasic region smectic-A + isotropic (S + I) where a GPTA-rich phase in the isotropic state coexists with a pure 8CB smectic-A phase. Below 85 wt % LC and upon heating a mixture in the S + I region, one observes a direct transition to a single isotropic phase. There is a sharp increase of the transition temperature from the smectic-A order to the isotropic state as the concentration of 8CB increases. Above 85 wt % LC and upon heating the system, the LC phase undergoes a transition from smectic-A to nematic and from nematic to isotropic state. The diagram indicates that the region where a nematic phase and an isotropic phase (N + I) coexist is quite small. This behavior is consistent with the results reported earlier on the mixture poly(styrene) (PS)/8CB in which the polymer is linear and has a molecular weight $M_w = 4000$ g/mol[27] although the latter system shows a lower miscibility. The phase behavior of the cured GPTA/8CB system is remarkably different from that of both uncured GPTA and linear PS/8CB systems as discussed in the forthcoming section.

Cured Samples. The experimental phase diagram of the cured GPTA/8CB mixtures is shown in Figure 2. This diagram exhibits a region where a smectic-A phase is in equilibrium with an isotropic phase, another region where a pure 8CB nematic phase coexists with a polymer-rich isotropic phase. In Figure 2, one also finds an isotropic miscibility gap in the upper range of 8CB composition above 40.5 °C and a single isotropic phase in the upper range of the temperature−composition diagram. With the present POM technique, it was possible to observe clearly the transition from N + I to isotropic phases above 30 wt % 8CB. Below this LC composition, the measurement shows no evidence of phase separation upon cooling the samples below 0 °C and slow heating. Transitions from S + I to N + I were observed in a limited range of LC weight fraction. The smectic-A LC domains coexisting with the polymer-rich isotropic phase are quite small, and their size shrinks significantly as the composition of 8CB decreases. Below 70 wt % 8CB, the POM observation of the transition from S + I to N + I was quite difficult and corresponded only to a change in the contrast within the sample. For this reason, we did not include the POM data for the transition temperature from S + I to N + I below 70 wt % 8CB.

The phase diagram of Figure 2 also shows the DSC data for the transition temperatures from smectic-A to nematic and from nematic to isotropic phases. The DSC

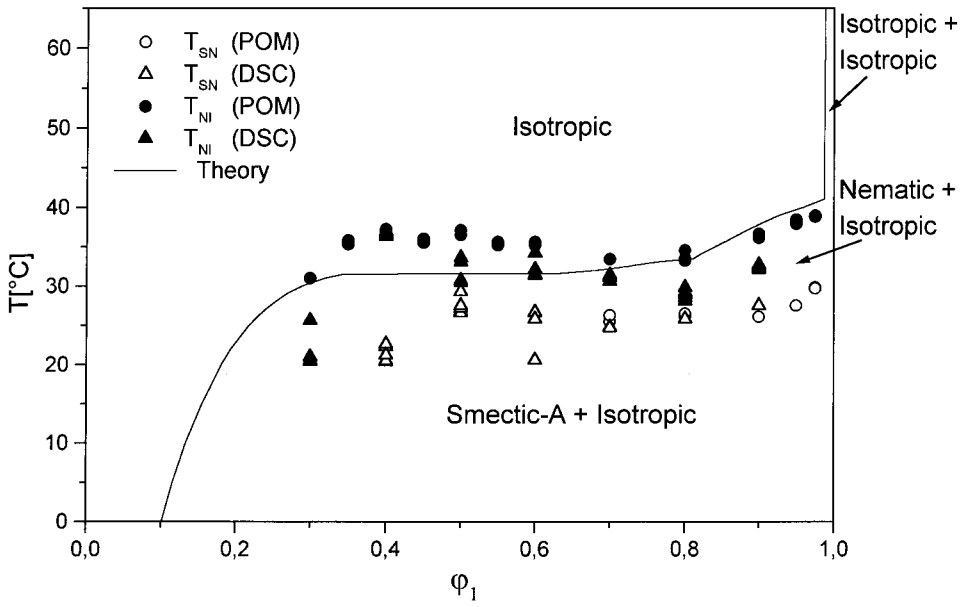

Figure 2. Diagram as in Figure 1 for the electron-beam cured mixtures. The model parameters employed in this case are $N_1 = 1$, $N_c = 50$, $\chi = -0.32 + 320/T + 0.7\varphi_2 + 0.03\varphi_2^2$, $T_{SN} = 33.5$ °C, $T_{NI} = 40.5$ °C, and $\zeta = 0.9375$.

and POM data are consistent over the whole range of composition covered by the experiments.

Comparison of Uncured and Cured Samples. The comparison between textures for uncured and cured systems is interesting. Micrographs in parts a and b of Figure 3 are taken on the uncured sample at the same composition, 95 wt % 8CB, and temperatures, $T = 20$ and 28 °C, respectively. Figure 3a corresponds to a temperature in the S + I region and exhibits the focal conic characteristic of the smectic-A texture. The isotropic phase is not seen in this micrograph because its polymer composition is low. Figure 3b displays the Schlieren texture characteristic of the nematic phase. Parts c and d of Figure 3 are taken on the cured sample at the same composition and the temperatures, $T = 20$ and 27 °C, respectively. Here, we clearly observe two coexisting phases. The dark regions represent the isotropic phase, and the others display the conic and fanlike texture typical of the smectic-A order. Note that the size of ordered domains is larger in the uncured samples.

A common feature of these diagrams is that the transition temperature obtained upon addition of a small amount of polymer to the pure LC decreases strongly. For example, in the uncured sample, the transition temperature T_{SN} at 90 wt % LC takes place at 23 °C, almost 10 °C below the transition temperature for pure 8CB. A similar decrease was observed for the transition temperature T_{NI}. Theoretically, the transitions from S + I to N + I and from N + I to I + I are horizontal lines at T_{SN} and T_{NI} of the pure LMWLC for both uncured and cured systems. These lines describe how the pure LC phase undergoes transitions from S to N and from N to I. There is a discrepancy between theory and experiments that will be discussed more in detail in a forthcoming paper. It is interesting to note that near the solubility limit of linear PS/8CB mixtures a decrease in the transition temperatures T_{SN} was also observed.[27] This decrease was more evident for low-molecular-weight PS, which is therefore close to the conditions of the uncured GPTA.

For cured samples, the decrease in the transition temperature T_{SN} extends to a lower LC composition. For instance, at 80 wt % LC, the T_{SN} transition temperature is 26 °C whereas for pure 8CB it is 33.5 °C, which means that the addition of 20 wt % GPTA results into a drop of the transition temperature by 7 °C. Such a behavior was not found in the case of linear PS/8CB mixtures, which exhibit remarkably different phase diagrams.[27] The transition temperature T_{SN} was the same as for the pure LC at all 8CB weight fractions. For linear polymer systems, the ordered domains were larger, and the contrast that takes place at the T_{SN} transition was observable at all compositions, as opposed to the case of the GPTA/8CB system.

In the phase diagram of the cured system (Figure 2), the solid line represents the theoretical prediction starting from the free energy of eq 2 for isotropic mixing and the Maier−Saupe−McMillan theory for nematic and smectic-A order. The parameters of rubber elasticity α and β are chosen according to the model of Petrovic et al.[13] The choice of these parameters is not crucial for the establishment of the phase diagram but allows improvement in the fitting procedure between the theory and experiments. The polymer volume fraction at cross-linking, φ_r, is identified with φ_2 because the films were prepared by a polymerization cross-linking process in the in situ situation, and therefore, one does not expect a noticeable change of the polymer volume fraction after the film is cured. To obtain a good fit with the data, it was necessary to allow the isotropic interaction parameter χ to be a function of the temperature and composition[28] according to $\chi = -0.38 + 320/T + 0.7\varphi_2 + 0.03\varphi_2^2$. This choice of parameters enabled us to fit the data reasonably well with $N_c = 50$. The variation of the interaction parameter χ with the composition was selected to capture the plateaulike behavior of data in the intermediate composition range, whereas N_c determines essentially the extent of the miscibility of the GPTA/8CB mixture in the isotropic state. The true value of N_c is certainly smaller than 50, the value used to fit the experimental data. This is probably due to the fact that the theoretical model is based on an ideal network description that does not take into account the defects and homogeneities inherent in real polymer networks.

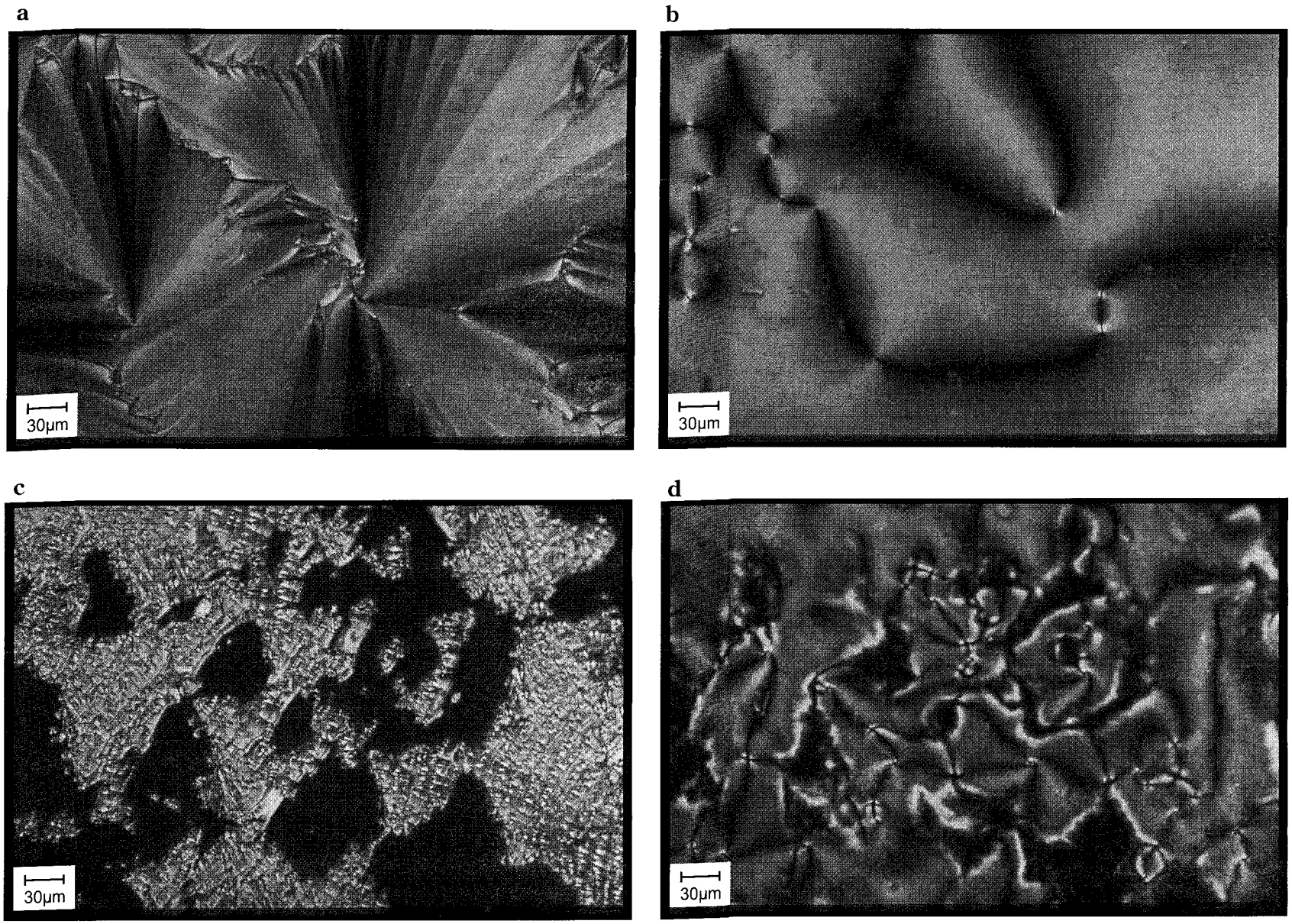

Figure 3. Optical micrographs taken at a liquid crystal weight fraction $\varphi_1 = 0.95$ and for (a) uncured sample at $T = 20$ °C showing the morphology in the smectic-A phase, (b) uncured sample at $T = 28$ °C showing the nematic texture, (c) cured sample at $T = 20$ °C showing coexisting smectic-A and isotropic phases, and (d) cured sample at $T = 27$ °C showing coexisting nematic and isotropic phases.

The elastic restoring forces at the cross-links put an upper bound on the swelling of the network. When the saturation limit is reached, a pure solvent phase appears and leads to the miscibility gap I + I above T_{NI}. This is different from the linear polymer systems where the emergence of the I + I region takes place only for systems with reduced miscibility. For example, in our recent study of the phase behavior of PS/8CB mixtures with three PS molecular weights M_w = 4000, 44 000, and 200 000 g/mol,[27] it was found that the blend with the lowest M_w did not show the I + I region because of enhanced miscibility, whereas blends with the latter two M_w did show I + I gaps. Therefore, unlike systems with linear polymers, mixtures of cross-linked networks and LMWLC always show an I + I region above T_{NI}. In Figure 2, the solid line going upward in the vicinity of the axis corresponding to pure LC is the theoretical prediction for $N_c = 50$, separating the isotropic miscibility gap I + I and the region of a single isotropic phase.

The analysis of the phase diagram of the uncured system is much simpler because it requires only the number of repeat units of GPTA and the variation of the χ-parameter with temperature. The solid line in Figure 1 represents the theoretical prediction based on a combination of the Flory−Huggins theory of isotropic mixing and the Maier−Saupe−McMillan theory for smectic-A and nematic order. The parameters used to fit the data here are $N_2 = 2$ and $\chi = -6.075 + 1861/T$. The agreement between theory and experimental data for this system is also quite good.

Conclusions

This work is an attempt to elucidate the phase behavior of cross-linked polymer and LMWLC. It combines experimental phase diagrams obtained by POM and DSC techniques and a theoretical framework based on classical meanfield theories. Cured and uncured systems are investigated to identify the effect of cross-links and are compared with results obtained previously with systems involving linear polymers. Therefore, cured GPTA/8CB samples covering the whole composition range of the phase diagram were prepared employing electron-beam irradiation.

The experimental phase diagram of GPTA/8CB mixtures in the uncured and in the cured state was constructed using POM and DSC measurements. The phase diagrams for the samples studied show several coexisting phases, including smectic-A, nematic, and isotropic phases. Comparison between uncured and cured systems exhibit a much higher miscibility of the uncured samples. An unusual decrease of transition temperatures from the smectic-A to nematic and from nematic to isotropic phases was observed. A possible explanation for this behavior in the case of the uncured system is suggested. The cured systems behave quite differently as compared to corresponding systems involving linear polymers. The coexisting curve for the cured system describing the transition from nematic to isotropic phases is described within the theoretical framework using the model for network elasticity and the Maier−Saupe−McMillan theories for smectic-A and nematic orders. For the uncured system, a similar procedure is used, and the isotropic part of the free energy is modeled within the Flory−Huggins theory. The agreement between the experimental data and the theory is good with a reasonable choice of parameters.

Acknowledgment. This work has been accomplished during a stay of F.B. at the Université du Littoral at Dunkerque (France) as a guest professor. The authors gratefully acknowledge the support of the C.N.R.S., the Région Nord-Pas de Calais, and the Ministère de l'Enseignement Supérieur et de la Recherche.

References and Notes

(1) De Gennes, P. G.; Prost, J. *The Physics of Liquid Crystals*; Oxford Science Publications: Oxford, 1995.
(2) Chandrasekhar, S. *Liquid Crystals*, 2nd ed.; Cambridge University Press: Cambridge, 1992.
(3) Drzaic, P. S. *Liquid Crystal Dispersions*; World Scientific: Singapore, 1995.
(4) Doane, J. W. Polymer Dispersed Liquid Crystal Displays. In *Liquid Crystals: Their Applications and Uses*; Bahadur, B., Ed.; World Scientific: Singapore, 1990.
(5) Maschke, U.; Coqueret, X.; Loucheux, C. *J. Appl. Polym. Sci.* **1995**, *56*, 1547.
(6) Maschke, U.; Coqueret, X.; Benmouna, M. *Polym. Networks Blends* **1997**, *7*, 23.
(7) Maschke, U.; Traisnel, A.; Turgis, J.-D.; Coqueret, X. *Mol. Cryst. Liq. Cryst.* **1997**, *299*, 371.
(8) Nwabunma, D.; Kim, K. J.; Lin, Y.; Chien, L. C.; Kyu, T. *Macromolecules* **1998**, *31*, 6806.
(9) Nwabunma, D.; Kyu, T. *Macromolecules* **1999**, *32*, 664.
(10) Flory, P. J.; Rehner, J. *J. Chem. Phys.* **1944**, *12*, 412.
(11) Treolar, L. R. G. *The Physics of Rubber Elasticity*, 3rd ed.; Clarendon Press: Oxford, 1975.
(12) Flory, P. J.; Erman, B. *Macromolecules* **1982**, *15*, 800.
(13) Petrovic, Z. S.; MacKnight, W. J.; Koningsveld, R.; Dusek, K. *Macromolecules* **1987**, *20*, 1088.
(14) Mishra, V.; Du Prez, F. E.; Gosen, E.; Goethals, E. J.; Sperling, L. H. *J. Appl. Polym. Sci.* **1995**, *58*, 331.
(15) Moerkerke, R.; Koningsveld, R.; Berghmans, H.; Dusek, K.; Solc, K. *Macromolecules* **1995**, *28*, 1103.
(16) Moerkerke, R.; Meeussen, F.; Koningsveld, R.; Berghmans, H.; Mondelaers, W.; Schacht, E.; Dusek, K.; Solc, K. *Macromolecules* **1998**, *31*, 2223.
(17) Maier, W.; Saupe, A. *Z. Naturforsch.* **1959**, *14A*, 882.
(18) Maier, W.; Saupe, A. *Z. Naturforsch.* **1960**, *15A*, 287.
(19) McMillan, W. L. *Phys. Rev. A* **1971**, *4*, 1238.
(20) Benmouna, F.; Bedjaoui, L.; Maschke, U.; Coqueret, X.; Benmouna, M. *Macromol. Theory Simul.* **1998**, *7*, 599.
(21) Benmouna, F.; Coqueret, X.; Maschke, U.; Benmouna, M. *Macromolecules* **1998**, *31*, 4879.
(22) Benmouna, F.; Maschke, U.; Coqueret, X.; Benmouna, M. *Macromol. Theory Simul.* **1999**, *8*, 479.
(23) Kyu, T.; Chiu, H.-W. *Phys. Rev. E* **1996**, *53*, 3618.
(24) Chiu, H.-W.; Kyu, T. *J. Chem. Phys.* **1997**, *107*, 6859.
(25) Chiu, H.-W.; Kyu, T. *J. Chem. Phys.* **1998**, *108*, 3249.
(26) Kyu, T.; Liang, S.; Chiu, H.-W. *Macromolecules* **1998**, *31*, 3604.
(27) Benmouna, F.; Daoudi, A.; Roussel, F.; Buisine, J.-M.; Coqueret, X.; Maschke, U. *Macromolecules*, accepted for publication.
(28) Koningsveld, R.; Kleintjens, L. A.; Shultz, A. R. *J. Polym. Sci., Part A-2* **1970**, *8*, 1261.

MA991389H